

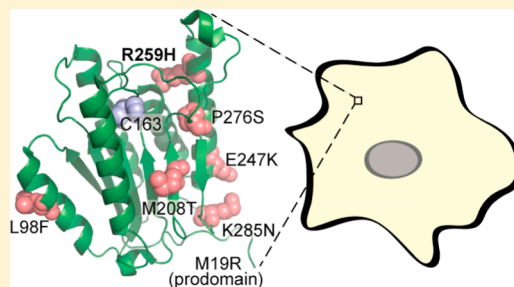
Tumor-Associated Mutations in Caspase-6 Negatively Impact Catalytic Efficiency

Kevin B. Dagbay, Maureen E. Hill, Elizabeth Barrett, and Jeanne A. Hardy*¹

Department of Chemistry, University of Massachusetts Amherst, Amherst, Massachusetts 01003, United States

Supporting Information

ABSTRACT: Unregulated, particularly suppressed programmed cell death is one of the distinguishing features of many cancer cells. The cysteine protease caspase-6, one of the executioners of apoptotic cell death, plays a crucial role in regulation of apoptosis. Several somatic mutations in the *CASP6* gene in tumor tissues have been reported. This work explores the effect of *CASP6* tumor-associated mutations on the catalytic efficiency and structure of caspase-6. In general, these mutations showed decreased overall rates of catalytic turnover. Mutations within 8 Å of the substrate-binding pocket of caspase-6 were found to be the most catalytically deactivating. Notably, the R259H substitution decreased activity by 457-fold. This substitution disrupts the cation- π stacking interaction between Arg-259 and Trp-227, which is indispensable for proper assembly of the substrate-binding loops in caspase-6. Sequence conservation analysis at the homologous position across the caspase family suggests a role for this cation- π stacking in the catalytic function of caspases generally. These data suggest that caspase-6 deactivating mutations may contribute to multifactorial carcinogenic transformations.



Caspases make up a family of cysteine-aspartic acid proteases that are critical to mediating programmed cell death and maintaining homeostasis within the cell. Caspases are synthesized as inactive procaspase zymogens consisting of a connected prodomain, a large subunit, an intersubunit linker region, and a small subunit (Figure 1A). Depending on their function within the apoptotic cascade, caspases are classified as initiators (caspase-2, -8, and -9) or executioners (caspase-3, -6, and -7).^{3,4} When the cell receives a death signal, either from cellular stress (intrinsic pathway) or from an extracellular death ligand (extrinsic pathway), initiator caspases are recruited to the apoptosome (caspase-9) or DISC complex (caspase-8) to begin the cascade.⁵ The constitutively dimeric executioner caspases are activated when they are cleaved at the intersubunit linker by the initiator caspases. Active executioner caspases cleave downstream substrates at specific aspartic acid residues, leading to a loss or gain of function of critical substrates. Both the extrinsic and intrinsic apoptotic pathways eventually lead to the destruction of the cell.⁶⁻⁹

Caspase-6 is expressed as an inactive zymogen that is activated by proteolytic processing at a conserved aspartate residue in the intersubunit linker [Asp-179 (caspase-3 processing) or Asp-193 (self-activation)] between the large and small subunits as well as before the prodomain.¹⁰ Caspase-6 is often activated by caspase-3 rather than by initiator caspases¹¹ and has been shown to undergo self-activation both *in vitro* and *in vivo*.^{12,13} Caspase-6 is less apoptotic than either caspase-3 or -7, each of which is directly processed by the initiators caspase-8 and -9.¹⁴ However, the overexpression of caspase-6 alone has been shown to promote cell death.¹⁵ Structurally, caspase-6 is most homologous to caspase-3 and

caspase-7 but has a preference for cleaving VEID motifs rather than the DEVD consensus sequence favored by caspase-3 and -7.¹⁶ Furthermore, caspase-6 has distinct substrates compared to other caspases, such as lamin A/C.¹⁷ An extensive analysis of caspase-2 and caspase-6 native substrates using MS-based proteomics revealed 204 unique caspase-6 substrates.¹⁸ Many caspase-6-specific substrates are known to be tumor-associated on the basis of their inclusion in the census of human cancer genes.¹⁹ Representative cancer-associated caspase-6 substrates include the double-strand-break repair protein, RAD21; cellular tumor antigen p53, TP53; the breast cancer type 1 susceptibility protein, BRCA1; the DNA repair protein complementing XP-G cells, ERCC5; the DNA mismatch repair protein, MLH1; and the Ras-related protein Rab-10, RB10. Thus, the crosstalk of caspase-6 with these known tumor-associated substrates suggests the potential involvement of caspase-6 in the development of cancer.

As mediators of apoptotic cell death, caspases natively play an essential role in preventing the development of cancer. Unregulated cell proliferation and a reduced apoptotic index are hallmarks of cancer. Inhibition of the caspases can lower the apoptotic index, thereby promoting tumorigenesis.²⁰ The development of inhibitory somatic mutations or a decrease in the expression of proapoptotic molecules could diminish the extent of cancer cell apoptosis by directly reducing caspase activity. In fact, somatic mutations in caspases have already

Received: April 19, 2017

Revised: July 18, 2017

Published: July 20, 2017

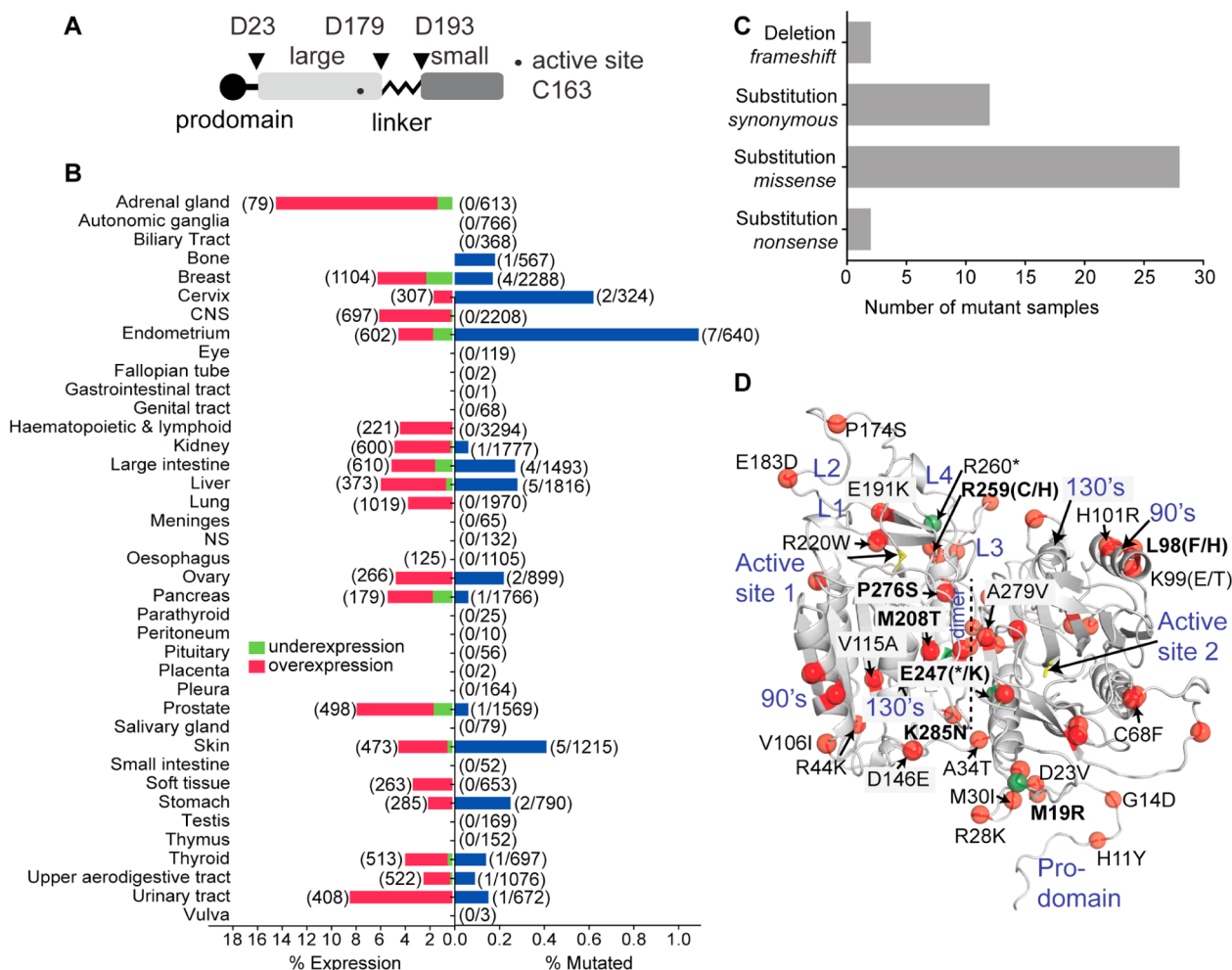


Figure 1. Tumor-associated mutations are widely distributed across caspase-6. (A) Linear cartoon of one monomer of procaspase-6 illustrating the prodomain (black circle), the large subunit (light gray box), the intersubunit linker (black zigzag), and the small subunit (dark gray box). The active site Cys-163 is denoted by a dot. Inverse triangles indicate proteolytic cleavage sites. (B) Aberrant *CASP6* gene regulation correlates with percent mutation in caspase-6 in tumor-associated tissue types. *CASP6* gene expression level in various tumor-associated tissues as catalogued from the COSMIC database. In parentheses is the total number of samples tested for a given tumor tissue type. Percentage *CASP6* gene expression (left) is presented as either underexpression (green) or overexpression (red). Percentage of samples with a mutated *CASP6* gene in tumor tissue type catalogued from the COSMIC database (blue). In parentheses is the fraction of the samples with mutations in the *CASP6* gene relative to the total number of samples (right). (C) Relative abundance of the types of mutations observed in the *CASP6* gene. (D) Observed tumor-associated nonsense (green sphere) and missense (red spheres) mutations in caspase-6 are mapped onto the model structure of full-length procaspase-6 with the active site cysteine drawn as yellow sticks. The attachment point for the prodomain is visible for only one of the monomers in this orientation. The model procaspase-6 structure was generated on the basis of zymogen structures 4IYR and 3NR2 with missing regions modeled *de novo*. Substrate-binding loops (L1–L4) along with key regions in caspase-6 (90s, 130s, and the active site) are also indicated. Highlighted in bold are the tumor-associated mutations interrogated in this study. An asterisk indicates the premature appearance of a stop codon characteristic of a nonsense mutation.

been identified in tumor-associated tissues.^{2,21–28} For example, *CASP8* somatic mutations were found in advanced gastric cancer carcinoma that significantly decreased caspase-8 apoptotic activity.²⁹ The well-known MCF-7 breast cancer cell line lacks caspase-3 expression because of a functional deletion mutation in the *CASP3* gene.³⁰ Importantly, these somatic mutations evidence a decrease in caspase activity when compared to that of the wild type and suggest that caspase inhibition may contribute to cancer pathogenesis.

In addition, caspase-6 showed differential gene regulation profiles in various tumor tissues, which have been tested and catalogued in the Catalogue of Somatic Mutations in Cancer (COSMIC database)¹ (Figure 1B). Both overexpression and underexpression of caspase-6 have been observed across various tumor tissues. For various tumor tissues, an aberrant gene

regulation profile usually correlates with the observations of a mutant *CASP6* genotype (Figure 1B). There were exceptions to this pattern, particularly in the tumor-associated samples from the adrenal gland, central nervous system (CNS), hematopoietic/lymphoid, lung, and the soft tissues, in which changes in gene regulation patterns did not correlate with enhanced mutational frequency in the *CASP6* gene. Furthermore, several *CASP6* mutations have been detected in tumor samples, constituting 0.13% of the total 29665 tumor tissue samples. While the identities of these mutations in *CASP6* in tumor tissues have been reported, the effect of each mutation on caspase-6 function is completely understudied. Together, these mutations and atypical gene expression profiles may implicate caspase-6 in tumorigenesis.

Perhaps because of its diminished apoptotic contribution, caspase-6 has not been as highly scrutinized for its role in cancer pathogenesis as other caspases. Initial work to compile a list of *CASP6* somatic mutations in tumor-associated tissues was reported more than a decade ago.² Three *CASP6* somatic mutations were detected in gastric and colorectal cancer tissues and were classified to be missense and nonsense mutations, but no studies reporting functional characterization of the proteins resulting from mutant *CASP6* have been reported. A search of the COSMIC database¹ revealed that caspase-6 harbored several mutations in tumor tissues. Of all reported mutations in *CASP6*, 64% resulted from missense mutations that encoded a different amino acid after a single-nucleotide change in the codon of the *CASP6* gene (Figure 1C). Caspase-6 also harbored functionally deleterious mutations, including deletions (frameshifts) and nonsense mutations resulting in the premature appearance of a stop codon within the *CASP6* gene. Interestingly, a significant fraction (27%) also showed synonymous substitution (silent) mutations. These tumor-associated mutations, with an emphasis on nonsense and missense mutations, are distributed across the structure of caspase-6, impacting regions both within the active site cavity and substrate-binding loops (Figure 1D) and outside, suggesting the potential of these mutations to modulate caspase-6 function.

To further explore the impact of somatic mutations on the function of caspase-6, tumor-associated variants were produced and tested in this study. *CASP6* somatic mutations identified from the COSMIC database¹ and from the initial *CASP6* mutational analysis study² were selected. *CASP6* mutations from the COSMIC database were chosen on the basis of their confirmed somatic status, their mutation type, and their varied structural location within the enzyme (Figure 1D). On the basis of these criteria, seven caspase-6 tumor-associated variants were generated with amino acid changes located in the prodomain, large subunit, and small subunit. This panel allowed us to explore the trend of somatic *CASP6* mutations in cancer pathogenesis and associated decreased apoptotic activity.

MATERIALS AND METHODS

Database Analysis of *CASP6* Gene Mutations. *CASP6* gene mutations in tumor samples were identified from the COSMIC database (<http://cancer.sanger.ac.uk/cosmic>)¹ and from a report of *CASP6* gene mutations in colorectal and gastric carcinomas.² Assessment of a total of 29815 sample tissues across all tumor-associated tissue types was reported for *CASP6* gene mutations. Representative missense mutations were selected on the basis of the locations of these mutations in the caspase-6 structure, which include the region of the prodomain (M19R), the 90s region (L98F), within the dimer interface (M208T and K285N), at the base of the helix adjoining L4 (E247K), and within an 8 Å radius of the active site Cys-163 (R259H and P276S). At the time we initiated this work, the M208T, E247K, and K285N mutations were present in the COSMIC database. These mutations were not present in the release of the COSMIC database available on the date of publication. On the basis of conversations with a curator at the COSMIC database, we came to understand that some of the data in the COSMIC database derive from the International Cancer Genome Consortium (ICGC). The ICGC freshly recompiles all of the data before each release of COSMIC. This means that all of the individual contributing laboratories are required to submit all of their data for each subsequent release.

If the lab no longer exists or forgets to submit data or if an analysis algorithm changes, legitimate data contained in a prior release may not appear in a current release. Thus, there are number of reasons that the caspase-6 mutations we have studied, M208T (COSM201127), E247K (COSM585487), and K285N (COSM345581), may not be included in the current ICGA release. In short, the absence of these mutations from the current release does not necessarily invalidate them.

Generation of Caspase-6 Tumor-Associated Variants.

The caspase-6 variants, full-length wild type (FL WT), FL C163S, and constitutively two-chain (CT) were derived from the synthetic, *Escherichia coli* codon-optimized (His)₆ C-terminally tagged caspase-6 gene (Celtek Bioscience) that was ligated into the NdeI/BamHI sites of the pET11a vector.³¹ Selected caspase-6 tumor-associated variants were generated using FL WT as the template through Phusion site-directed mutagenesis (Thermo Scientific). The caspase-6 R259H CT and W227A CT variants were particularly generated using caspase-6 D179CT as the template for the site-directed mutagenesis.

Caspase-6 Protein Expression and Purification.

Caspase-6 expression constructs were transformed into the BL21(DE3) T7 express strain of *E. coli* (New England Biolabs). Overnight seed cultures were initially grown in 2xYT medium supplemented with 0.1 mg/mL ampicillin (Sigma) at 37 °C. Dense cultures were then diluted 1000-fold with 2xYT medium containing 0.1 mg/mL ampicillin and shaken at 37 °C until the A₆₀₀ reached 0.6. Protein expression was induced by the addition of 1 mM isopropyl 1-thio-β-D-galactopyranoside, and cultures were shaken at 20 °C for 18 h. Cells were centrifuged at 4700g for 10 min at 4 °C and stored at -20 °C until they were used. Frozen and thawed cells were lysed using a microfluidizer (Microfluidics, Inc.) in lysis buffer [50 mM Tris (pH 8.5), 300 mM NaCl, 5% glycerol, and 50 mM imidazole] and centrifuged at 30600g for 1 h at 4 °C. The supernatant was loaded into a 5 mL HiTrap nickel affinity column (GE Healthcare) and washed with lysis buffer until the absorbance returned to baseline levels. These proteins were eluted with elution buffer [50 mM Tris (pH 8.5), 300 mM NaCl, 5% glycerol, and 250 mM imidazole] and diluted 5-fold with buffer A [20 mM Tris (pH 8.5) and 2 mM DTT] to reduce the salt concentration. These protein samples were then loaded into a 5 mL HiTrap Q HP column (GE Healthcare). The chromatographic separations were performed with a linear NaCl gradient, and each protein was eluted in 20 mM Tris (pH 8.5), 200 mM NaCl, and 2 mM DTT. These eluted proteins were stored at -80 °C until they were used. Purified caspases were analyzed by sodium dodecyl sulfate–polyacrylamide gel electrophoresis (SDS–PAGE) to confirm their identity and purity.

Caspase-6 Activity Assays. To measure caspase-6 activity, the activity of 100 nM purified caspase-6 (WT and tumor-associated variants) was assayed over 7 min at 37 °C in caspase-6 activity assay buffer (100 mM HEPES, 120 mM NaCl, 0.1% CHAPS, 10% sucrose, and 5 mM DTT). For substrate titration, a range of 0–500 μM fluorogenic substrate VEID-AMC [*N*-acetyl-Val-Glu-Ile-Asp-(7-amino-4-methyl-coumarin), Enzo Life Sciences Inc.] was used. Fluorescence kinetic measurements ($\lambda_{\text{ex}} = 365$ nm, and $\lambda_{\text{em}} = 495$ nm) were performed as two independent trials on two separate days in 100 μL reaction mixtures in a 96-well format using a microplate reader (SpectraMax M5, Molecular Devices). Initial velocities versus substrate concentration were fit to a rectangular hyperbola

using GraphPad Prism (GraphPad Software, San Diego, CA) to determine kinetic parameters K_M and k_{cat} . Enzyme concentrations were determined by active site titration with the quantitative covalent inhibitor VEID-CHO (*N*-acetyl-Val-Glu-Ile-Asp-aldehyde, Enzo Life Sciences Inc.). Caspase-6 was added to the inhibitor solvated in dimethyl sulfoxide in 96-well V-bottom plates at room temperature for 1.5 h in caspase-6 activity assay buffer. Aliquots (90 μ L) were transferred in duplicate to black-well plates and assayed with a 50-fold molar excess of the substrate. The protein concentration was determined to be the lowest concentration at which full inhibition was observed and was thus used to calculate k_{cat} .

Self-Proteolysis Assay of Caspase-6 Tumor-Associated Variants. Caspase-6 variants (3 μ M) were allowed to self-cleave in caspase-6 activity assay buffer [100 mM HEPES (pH 7.5), 10% sucrose, 0.1% CHAPS, 120 mM NaCl, and 5 mM DTT] at 37 °C for 24 h. SDS loading buffer was added to the samples and boiled for 10 min prior to analysis by 16% SDS-PAGE. The gels were imaged using a ChemiDoc MP imaging system (Bio-Rad).

Proteolysis of Procaspase-6 FL C163S Protein by Caspase-6 Tumor-Associated Variants. Catalytically inactive procaspase-6 FL C163S (3 μ M) was incubated with each of caspase-6 tumor-associated variant (0.3 μ M) in caspase-6 assay buffer [100 mM HEPES (pH 7.5), 10% sucrose, 0.1% CHAPS, 120 mM NaCl, and 5 mM DTT] at 37 °C for a predetermined time interval. SDS loading buffer was added to the samples and boiled for 10 min prior to analysis by 16% SDS-PAGE. The gels were imaged using a ChemiDoc MP imaging system (Bio-Rad).

Intrinsic Fluorescence Spectroscopy. Caspase-6 tumor-associated variants (3 μ M) in 20 mM phosphate buffer (pH 7.5), 120 mM NaCl, and 2 mM DTT were prepared. Fluorescence emission scans (305–400 nm) were collected after excitation at 280 or 295 nm using a J-1500 spectrometer (Jasco) equipped with a fluorescence emission monochromator (FMO-522) and a detector (FDT-538). The signal was acquired by setting the emission detector at a high-tension voltage value of 700 V, the data integration time (DIT) to 1 s, and the data pitch to 1 nm. The bandwidths used for excitation and emission were 2 and 10 nm, respectively.

Caspase-6 Full-Length Structural Model Generation. The full-length caspase-6 zymogen model (residues 1–293) shown in Figure 1D was built from crystal structures of the caspase-6 zymogen. In our model, chain A was derived from Protein Data Bank (PDB) entry 4IYR (chain A); chain B of this model was derived from PDB entry 3NR2 (chain A) as templates. The missing residues [[1–30, 174–186, and 292–293] in PDB entry 4IYR (chain A); [1–30, 167–186, 261–271, and 292–293] in PDB entry 3NR2 (chain A)] were built by *de novo* modeling using Chimera/Modeller platforms.^{32,33} All illustrations with molecular visualization were generated using the PyMOL Molecular Graphics System (Schrödinger, LLC).

RESULTS AND DISCUSSION

Caspase-6 Mutants Identified in Tumor Tissues Have Decreased Activity. To further investigate the effect of these mutations on caspase-6 function, seven caspase-6 tumor-associated mutations were selected on the basis of their distribution across the caspase-6 structure (highlighted in bold in Figure 1D). All selected CASP6 mutations had a confirmed somatic (nongermline) status, and we focused our interrogation

on less conservative mutations. Representative missense mutations were selected from within the region of the prodomain (M19R), the 90s helix (L98F), within the dimer interface (M208T and K285N), at the base of the helix adjoining L4 (E247K), and within an 8 Å radius of the active site Cys-163 (R259H and P276S). At the time of publication, the M208T, E247K, and K285N mutations had been removed from the COSMIC database for unknown reasons (see Materials and Methods). The caspase-6 variants were expressed in *E. coli* and purified. The activities of the caspase-6 tumor-associated variants were assessed using a fluorogenic peptide-based substrate, VEID-AMC (Table 1). These variants were

Table 1. Kinetic Parameters^a of Selected Caspase-6 Tumor-Derived Variants Identified from the COSMIC Database¹ and Other Sources²

caspase-6 variant	K_M (μ M)	k_{cat} (s^{-1})	$\times 10^3 k_{cat}/K_M$ ($M^{-1} s^{-1}$)	x-fold decrease in turnover vs WT
WT	34 \pm 3.6	1.1 \pm 0.03	32	1
M19R	163 \pm 19	0.80 \pm 0.04	5.0	6.40
L98F	46 \pm 4.2	0.68 \pm 0.02	15	2.10
M208T	170 \pm 12.0	1.5 \pm 0.04	8.8	3.60
E247K	84 \pm 10	1.6 \pm 0.06	19	1.70
P276S	314 \pm 26	0.57 \pm 0.02	1.8	18.0
R259H	577 \pm 135	0.04 \pm 0.01	0.07	457
K285N	50 \pm 4.0	0.18 \pm 0.01	3.6	8.90
W227A	ND ^b	ND ^b	ND ^b	ND ^b

^aKinetic parameters of caspase-6 tumor-associated variants were determined using fluorogenic substrate VEID-AMC using 100 nM enzyme in caspase-6 activity assay buffer. The error represents the standard error of the mean (SEM) of two independent experiments.

^bNot detectable.

observed to have 2–457-fold decreases in catalytic efficiency compared to that of the wild type (WT) caspase-6. Mutations within the substrate-binding groove, P276S and R259H, had the most negative impact on caspase-6 activity. The decrease in the catalytic efficiency of all the caspase-6 tumor-associated variants against peptide-based substrates suggests that the mutations have caused changes in the structure or dynamics that result in less effective substrate catalysis.

Caspase-6 is the sole caspase for which a mechanism for intramolecular self-cleavage has been observed.^{12,13} As is the case under certain conditions in mammalian systems, during bacterial expression, WT caspase-6 is capable of self-maturation.³⁴ All of the caspase-6 tumor-associated variants were overexpressed in *E. coli* for 18 h at 20 °C and purified in the same manner (described in Materials and Methods). These expression conditions led to various extents of self-activation of WT and mutant caspase-6, as evidenced by the appearance of the large and small subunits following cleavage at D193, which is the activating event. Typically, caspase-6 is proteolytically cleaved at three sites to reach full maturation: one site in the prodomain (Asp-23) and two sites (Asp-179 and Asp-193) flanking the linker region (Figure 1A). In the context of cancer, the crucial activating event is cleavage at Asp-193. Complete removal of the intersubunit linker following cleavage at Asp-179 has no additional impact on measured catalytic function. Similarly, removal of the prodomain also does not impact catalytic activity.³¹

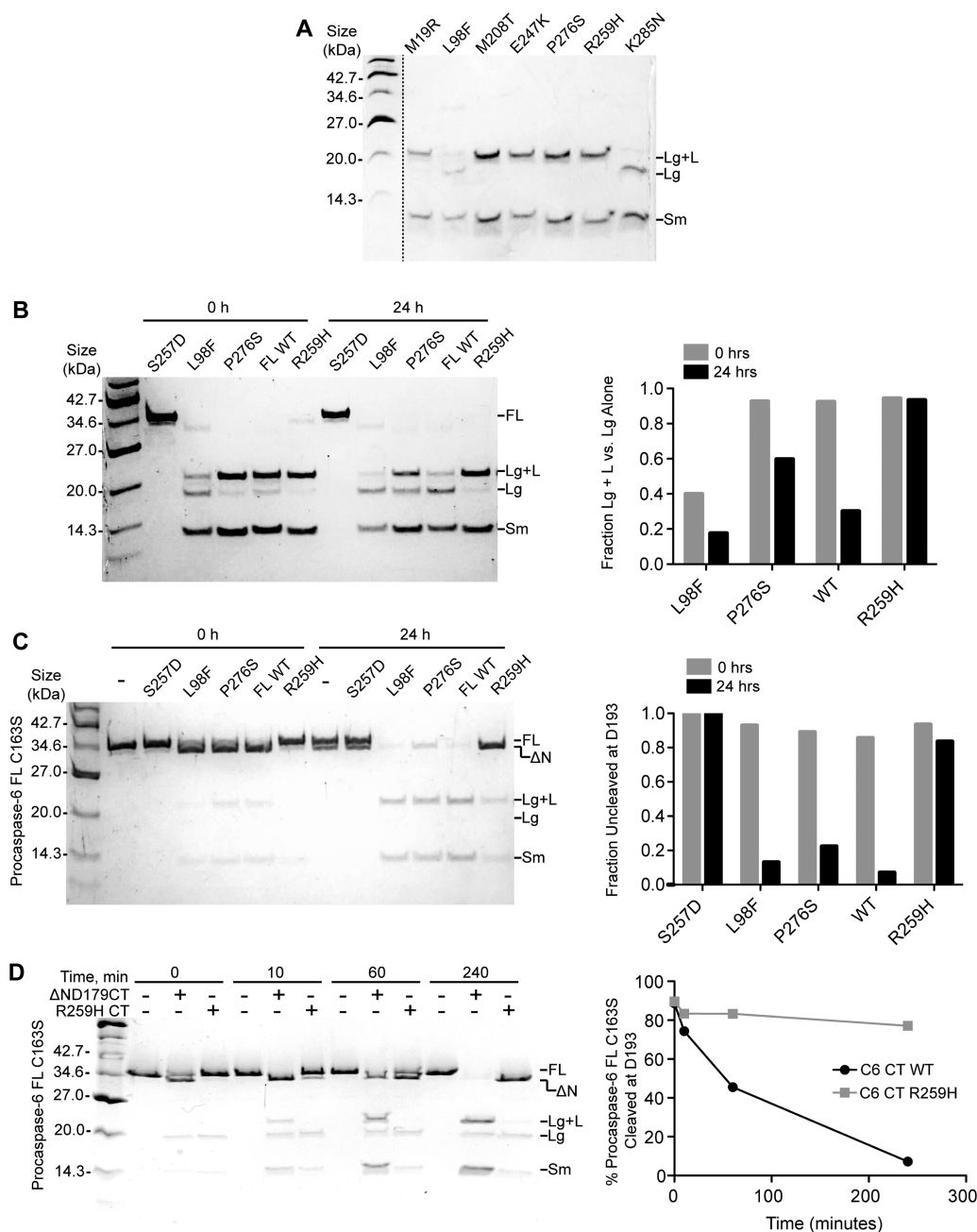


Figure 2. Most caspase-6 tumor-associated variants showed decreased proteolytic activity for self-processing and protein substrates. (A) Cleavage pattern of caspase-6 tumor-associated variants expressed in *E. coli* and purified to homogeneity. All caspase-6 tumor-associated mutations were introduced into the full-length (FL) caspase-6 wild type (WT) construct in a pET11a bacterial expression vector. Active procaspases self-process at Asp-193 to generate the large subunit with the intersubunit linker attached (Lg+L) and the small subunit (Sm). Subsequent cleavage at Asp-179 results in removal of the intersubunit linker to generate the large subunit (Lg). Concomitant cleavage at Asp-23 results in removal of N-terminal prodomain (Δ N) residues 1–23. (B) Self-cleavage pattern of recombinant caspase-6 tumor-associated variants (3 μ M) before and after a 24 h incubation in caspase-6 activity assay buffer at 37 $^{\circ}$ C (left) and the associated quantification (right). (C) Proteolysis of catalytically inactive procaspase-6 C163S (3 μ M) by caspase-6 tumor-associated variants (0.3 μ M) before and after a 24 h incubation in caspase-6 activity assay buffer at 37 $^{\circ}$ C (left) and the associated quantification (right). (D) Proteolysis of catalytically inactive procaspase-6 C163S (3 μ M) by caspase-6 tumor-associated variant R259H CT (0.3 μ M) or the wild type constitutively two-chain (WT CT or Δ ND179CT) after incubation in caspase-6 activity assay buffer at 37 $^{\circ}$ C for the indicated times (left) and the quantification (right). Two-chain forms of the mature wild type (WT CT) and R259H CT caspase-6 variants were generated to allow independent expression of the large and small subunits without the need for proteolytic cleavage for its activation.

All caspase-6 cancer mutants were able to undergo self-activation, though L98F and K285N were able to cleave their own intersubunit linker at Asp-179 at a rate even faster than that of the WT (Figure 2A). While this increase in activity can be observed for self-processing, it appears that it may not be

more rapid in the context of caspase-6 activity toward peptide substrates (Table 1) or protein substrates (Figure 2C).

The caspase-6 tumor-associated variants expressed from the gene for full-length caspase-6 were allowed to undergo self-proteolysis *in vitro* by a 24 h incubation in caspase-6 activity

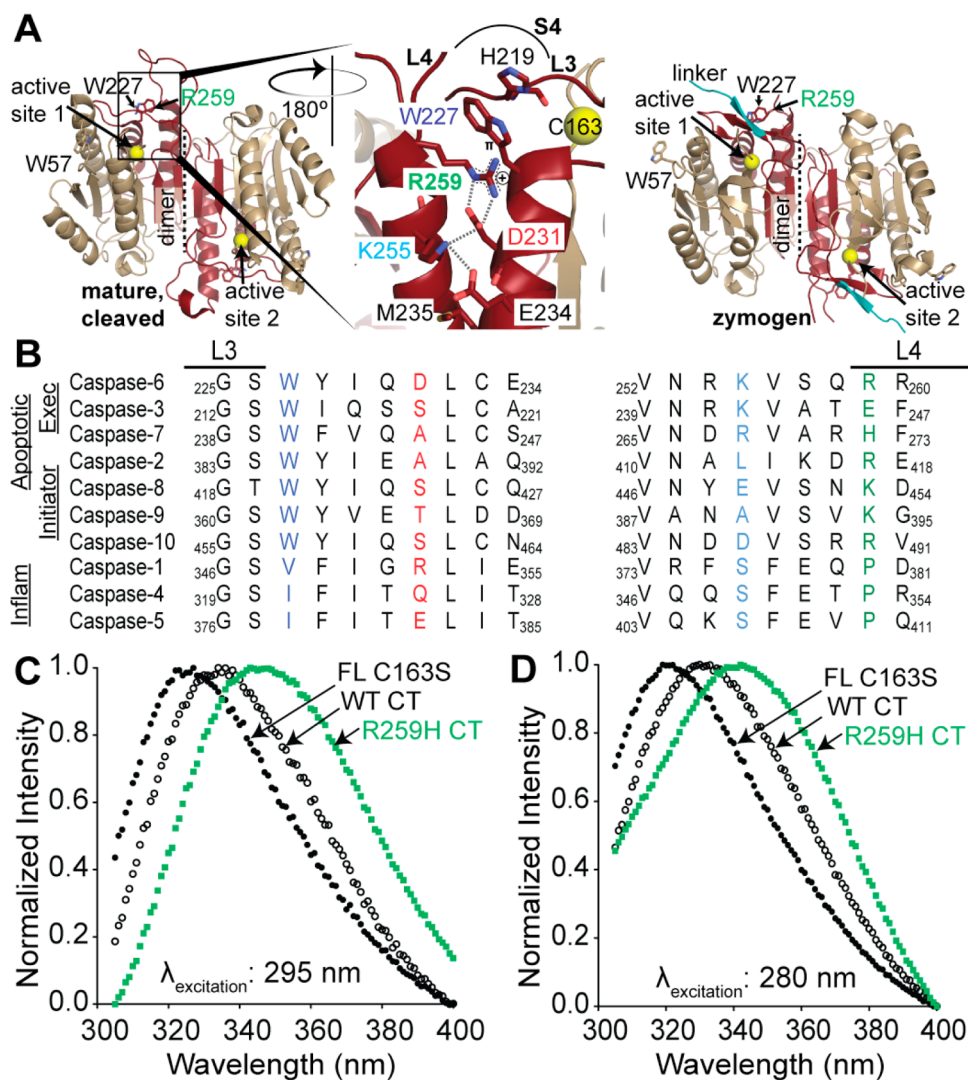


Figure 3. R259H disrupts interactions that are necessary for proper assembly of the substrate-binding groove. (A) Crystal structure of the mature, fully cleaved, unliganded caspase-6 (PDB entry 2WDP) (left). The locations of Arg-259, the active site Cys-163, and the two tryptophan residues (Trp-57 and Trp-227) in caspase-6 are indicated. The inset highlights the cation- π stacking and networks of H-bond interactions in which Arg-259 is involved, as well as the substrate-binding loops (L3 and L4) and substrate-binding pocket (S4) (middle). The crystal structure of the procaspase-6 zymogen (PDB entry 3NR2) and the location of Arg-259, Trp-57, Trp-227, and the intersubunit linker (cyan) are indicated (left). (B) Amino acid sequence alignment of key residues within the network of interactions of Arg-259 across the caspase family, including both apoptotic and inflammatory caspases. (C) Intrinsic tryptophan fluorescence profiles of full-length procaspase-6 C163S, caspase-6 CT, and caspase-6 R259H CT. Excitation at 295 nm primarily probes the polarity of the tryptophan microenvironment. (D) Intrinsic fluorescence profiles of caspase-6 variants excited at a 280 nm wavelength. Excitation at 280 nm probes the polarity of the microenvironment of all aromatic residues in a protein, including tryptophan, tyrosine, and phenylalanine.

assay buffer at 37 °C (Figure 2B). As expected, the full-length wild type (FL WT) caspase-6 showed a higher fraction of the fully cleaved large and small subunits, indicating close to full maturation. The caspase-6 phosphomimetic variant, S257D, is a surrogate of a phosphorylated caspase-6 at position 257. The S257D substitution is inactivated because of a misaligned substrate-binding groove in the crystal structure of this variant of caspase-6³⁴ and, correspondingly, showed no further cleavage into its large and small subunits (Figure 2B). L98F showed a cleavage pattern similar to that of the FL WT at 24 h, suggesting that the L98F mutation did not dramatically impact the self-cleavage activity over this time course. R259H and P276S showed higher fractions of large subunits with an attached intersubunit linker, a cleavage pattern different from those of the FL WT and L98F, which indicates that these

variants have somewhat slowed self-cleavage activity. Thus, the accessibility of the intersubunit linker to caspase-6 appears to be different in both P276S and R259H, perhaps suggesting an altered geometry of the substrate-binding cleft, generating a less proteolytically active enzyme.

The *trans* (intermolecular cleavage) activities of selected caspase-6 tumor-associated variants were tested using procaspase-6 FL C163S, a catalytically inactive variant of caspase-6, as a protein substrate (Figure 2C). Consistently, both P276S and R259H showed less proteolytic activity against this protein substrate than L98F and WT caspase-6 (Figure 2C). R259H emerged as the least active variant in cleaving procaspase-6 FL C163S, underscoring the severity of the impact of this mutation on the proper assembly of the substrate-binding cavity for efficient proteolysis. As the most inactive of the caspase-6

tumor-associated variants in cleaving both peptide-based and protein substrates, we sought to assess whether the R259H mutation impacted function in a homogeneous preparation of the fully mature form of caspase-6. To achieve this, the R259H mutation was then introduced into a constitutively two-chain (CT) caspase-6 expression construct³¹ which allows independent expression of the large and small subunits, mimicking a fully cleaved and mature caspase-6. The two-chain R259H CT is dramatically inactivated for cleavage of protein substrates compared to the mature, two-chain (CT) wild type (WT) caspase-6. This result further suggests that the R259H mutation negatively impacts the activity of the mature (cleaved) caspase-6 in cleaving protein substrates (Figure 2D). Together, these data suggest that the majority of inactivating mutations in caspase-6 found in tumor-associated tissues may have acquired a misaligned substrate-binding cleft or other defect-introducing structural changes that decrease the caspase-6 catalytic efficiency. Thus, it appears that the impairment of caspase-6 function in tumors need only prevent caspase-6 activity against other substrates, whereas self-cleavage poses no significant threat to the viability (apoptosis avoidance) of the cancer cells. This is consistent with our emerging understanding of caspase-6 activation. We hypothesize that procaspase-6 self-activation is critical in a neurodegenerative context, but activation by upstream caspases is critical for apoptosis.

Caspase-6 R259H Disrupts an Interaction That Is Necessary for Proper Assembly of the Substrate-Binding Groove. R259H is the most inactivating mutation among caspase-6 tumor-associated variants we analyzed. To further understand the impact of the R259H substitution on the proper assembly of the substrate-binding groove, the crystal structure of active, mature caspase-6 (PDB entry 2WDP) was further inspected. Arg-259, which is located at the base of L4, is part of a network of H-bond and cation- π stacking interactions (Figure 3A) that provides a stable foundation for proper assembly of substrate-binding loops and is therefore essential for the establishment of a catalytically competent caspase-6. The usually positively charged guanidinium group of arginine exhibits a strong propensity to stack against aromatic residues and is also capable of H-bonding to neighboring oxygen atoms.³⁵ In caspase-6, Arg-259 forms two H-bonds with Asp-231 and interacts with Trp-227 through cation- π stacking, as predicted by the CAPTURE analysis that can identify energetically significant cation- π interactions.³⁶ In addition, Trp-227 also holds L3 in place through a cation- π stacking interaction with His-219, underscoring its importance in situating the active site loop bundle. Mutating Trp-227 to alanine produced a predominantly inactive, full-length caspase-6 (Figure S1A) that was incapable of self-cleavage even after incubation for 24 h at 37 °C (Figure S1B). To assess its ability to cleave other substrates, W227A was expressed in the mature, constitutively two-chain version of caspase-6 using the CT construct. Caspase-6 W227A CT was unable to cleave the fluorogenic peptide substrate VEID-AMC (Table 1), demonstrating that this substitution is deleterious to both self-activation in *cis* and cleavage of other substrates in *trans*. This strongly suggests that the interaction of Arg-259 with Trp-227 through cation- π stacking is critical for function. Both residues Arg-259 and Trp-227 are part of the cluster that forms the S4 substrate-binding pocket in caspase-6. This cation- π interaction (Arg-259 and Trp-227 in caspase-6) is conserved in six of the seven apoptotic caspases but not in the inflammatory caspases (Figure 3B). Thus, this interaction may also be used

by other apoptotic caspases to stabilize the substrate-binding groove for efficient substrate binding and catalysis. On the other hand, the position of Asp-231 is not conserved across the caspase family, so the two H-bonds between Arg-259 and Asp-231 are unique to caspase-6. These residues also form a salt bridge, which would additionally be disrupted by the R259H mutation. Thus, the Arg-259 mutation is likely to impact caspase-6 through disruption of two critical interactions with Trp-227 and Asp-231. One might expect, on the basis of this analysis, that tumor-associated mutations might occur at Trp-227 and Asp-231. To date, no tumor-associated mutations have been observed at any of these three positions (Trp-227, Asp-231, and Arg-259; caspase-6 numbering); however, this may be simply due to incomplete coverage of all tumor genotypes.

The intrinsic fluorescence properties of Trp-227 allow this residue to function as a sensitive probe for the cation- π stacking interaction between Arg-259 and Trp-227 and the other network of interactions that give rise to the proper assembly of the substrate-binding groove. Caspase-6 has only two Trp residues, which are both located in substrate-binding loop L1 (Trp-57) and at the base of loop L4 (Trp-227), which is directly adjacent to Arg-259. Trp-57 in both the zymogen and active forms is constantly solvent-exposed, while the micro-environment of Trp-227 varies between these forms of caspase-6 (Figure 3A). Thus, intrinsic tryptophan fluorescence could likely report the relative microenvironment of Trp-227 in the absence and presence of the R259H mutation and, in turn, provides structural hints about the proper assembly of the substrate-binding groove in caspase-6. Intrinsic tryptophan fluorescence is dependent on the polarity of the environment, where shifts in the maximum emission toward longer wavelengths (red shift) indicate a higher degree of solvent exposure. Intrinsic fluorescence spectra were collected from caspase-6 variants, including the catalytically inactive procaspase-6 FL C163S, the mature caspase-6 (CT), and the mature caspase-6 R259H (CT).

As expected, upon specific tryptophan excitation at 295 nm (Figure 3C), the procaspase-6 zymogen showed a 10 nm shift in maximum emission toward a shorter wavelength (blue shift) compared to the two-chain mature caspase-6 wild type (CT), suggesting a less solvent-exposed Trp-227 microenvironment. In the procaspase-6 zymogen structure (Figure 3A), the intersubunit linker sits on top of the substrate-binding groove in the procaspase-6 zymogen, restricting the solvent accessibility of Trp-227, which is one of the critical residues in the substrate-binding pocket of caspase-6. Meanwhile, the R259H CT variant displayed a significantly extended 12 nm shift in maximum emission toward a longer wavelength (red shift) compared to caspase-6 CT, indicating a highly solvent-exposed Trp-227 microenvironment. A similar trend was observed with 280 nm excitation of all aromatic residues (Trp, Tyr, and Phe) (Figure 3D). Thus, the change in the polarity of the Trp-227 microenvironment in the presence of the R259H mutation in caspase-6 suggests a disruption of the stabilizing cation- π stacking interaction of Arg-259 with Trp-227. It further disrupts the networks of H-bonding interactions that results in misaligned loops in the substrate-binding pocket, rendering it incapable of the efficient catalytic turnover of substrates.

CONCLUSIONS

This study demonstrates that all of the selected mutations in caspase-6 found in several tumors resulted in an overall decrease in the catalytic efficiency of caspase-6. The fact that

Table 2. Identified Missense and Nonsense Mutations in Caspase-6 from Various Tumor Tissue Types and Their Corresponding Tissue Distribution^a

mutation	tissue	histology	other caspase mutations ^e	ref
H11Y	prostate	carcinoma	none	49
G14D	skin	carcinoma	none	50
M19R	ovary	carcinoma	none	CGARN ^e , ⁵¹
D23V	bone	Ewings sarcoma	none	52
R28K	skin	carcinoma	caspase-8 (S33F, S375F)	53
M30I	endometrium	carcinoma	caspase-2 (A259A)	1
A34T ^c	endometrium, stomach	carcinoma	caspase-3 (L118I, D192N), caspase-4 (R55W), caspase-10 (E22D), caspase-14 (E49K)	1
R44K	colon	carcinoma	caspase-3 (F193L), caspase-8 (R162I)	2
C68F	kidney	carcinoma	none	54
L98F	endometrium	carcinoma	caspase-1 (frameshift)	1
L98H	thyroid	carcinoma	none	1
K99E ^{c,d}	liver	carcinoma	none	1
K99T	cervix	carcinoma	caspase-8 (N197T), caspase-14 (Q70K)	1
H101R ^{c,d}	liver	carcinoma	none	1
V106I	cervix	carcinoma	none	1
V115A	stomach	carcinoma	caspase-5 (frameshift)	55
D146E	liver	carcinoma	none	1
P174S	skin	carcinoma	none	53
E183D ^d	endometrium	carcinoma	caspase-7 (K109N), caspase-8 (R52I, R111I, T461P, T503P)	1
E191K	urinary tract	carcinoma	none	1
M208T	large intestine	carcinoma	none	1
R220W	endometrium	carcinoma	caspase-2 (L232R, R417W, L125F), caspase-3 (R207 ^b), caspase-4 (V252I), caspase-5 (Y87 ^b , Y116 ^c)	1
E247K	lung	carcinoma	none	1
E247 ^b	breast	carcinoma	caspase-4 (E351A), caspase-8 (D73A, D132A, E399 ^b , E441 ^b)	1
R259C	endometrium	carcinoma	caspase-1 (G85W), caspase-2 (A412V), caspase-4 (K42Q), caspase-7 (T18A), caspase-8 (E36 ^b , E95 ^b)	1
R259H	colon	carcinoma	none	2
R260 ^b	large intestine	carcinoma	none	1
P276S	breast	carcinoma	none	1
A279V ^d	endometrium	carcinoma	caspase-7 (K109N), caspase-8 (R52I, R111I, T461P, T503P)	1
K285N	lung	carcinoma	none	1

^aData were pooled from the COSMIC database¹ and from a reported *CASP6* mutational study.² Highlighted in bold are the specific caspase-6 tumor-associated variants interrogated in this study. ^bNonsense mutations. ^cMutation found in two separate samples. ^dMutations found in the same sample ID. ^eOther caspase mutations found in the same sample ID.

all of the selected mutations in all regions of caspase-6 had functional impacts strongly suggests that decreasing the caspase-6 intrinsic activity via the introduction of somatic mutations is helpful in establishing a tumorigenic phenotype. In particular, R259H was found to be severely deactivating via a mechanism that disrupts cation- π stacking and the networks of H-bonding interactions necessary for the proper alignment of loops in the substrate-binding groove of caspase-6.

One would anticipate that mutations in caspases would decrease the apoptotic potential of the cells containing mutant caspases. Neutralizing/inactivating mutations in caspase-6 should therefore play a role in tumorigenesis. For example, caspase-6 is a direct activator of the initiator caspase-8.³⁷ Thus, in a cellular context, activation through caspase-6 presents one of the regulatory pathways of caspase-8. *CASP8* is a tumor-associated gene, and its polymorphisms are correlated with an increased risk of various types of cancer.^{38–41} In addition to its central role in apoptosis, caspase-8 has emerging nonapoptotic roles in cells such as potentiating NF- κ B signaling,⁴² regulating autophagy,⁴³ and cellular adhesion and migration.^{44,45} Thus, regulation of caspase-6 may possibly impact both the apoptotic and the nonapoptotic tumor-associated roles of caspase-8,

suggesting another possible mechanism by which caspase-6 can play a role in tumor development. While these data suggest that caspase-6 mutations contribute to development of a cancerous phenotype, we do not anticipate that mutations in caspase-6 alone would be sufficient to cause cancer independently. In fact, a recent analysis of genetic variations of more than 60000 exomes found a rare R259H-encoding allele of caspase-6.⁴⁶ It is likely that caspase-6 mutations act in concert with many other mutant alleles, ultimately contributing to a cancerous condition. Therefore, R259H alone could be present in many healthy cells but may predispose individuals to certain types of cancer.

Together with the aberrant regulation of caspase-6, some tumor samples that harbored *CASP6* gene mutations also contained mutations in other caspases (Table 2). Particularly interesting is the coexistence of mutations in the initiator *CASP8*, a known oncogene,⁴⁷ where 24% of the tumor samples with *CASP6* mutations also harbored *CASP8* mutations. The co-occurrences of mutations in multiple caspases may be expected and underscore the complexity of each individual event of tumorigenesis. This may suggest the existence of altered regulation of the apoptotic cascade or other non-

apoptotic pathways relevant to the evolution of a tumor phenotype.

The fact that several different mutations in different regions of caspase-6 were observed in different tumors suggests the possibility that unique contributions of various aspects of caspase-6 function may be at play in different cancers. The roles of each component in the pathway to tumor development will enable a better understanding of the controlling factors that allow the misregulation observed in cancer cells of many varieties. This work demonstrates that in cases in which caspase-6 is mutated in tumors, significant impacts on catalytic function are observed. What remains to be seen is whether other aspects of caspase-6 regulation, such as post-translational modifications, dynamics, and substrate selection, are likewise impacted by these tumor-associated mutations. One might envision that delivery of WT caspases, as we have recently demonstrated,⁴⁸ might allow recovery of the deficiencies in caspase-6 activity.

■ ASSOCIATED CONTENT

■ Supporting Information

The Supporting Information is available free of charge on the ACS Publications website at DOI: 10.1021/acs.biochem.7b00357.

Purification gel of caspase-6 FL W227A and self-cleavage assay of caspase-6 FL W227A before and after a 24 h incubation at 37 °C (Figure S1) (PDF)

■ AUTHOR INFORMATION

Corresponding Author

*Department of Chemistry, University of Massachusetts Amherst, 745A Lederle Graduate Research Tower, 710 N. Pleasant St., Amherst, MA 01003. E-mail: hardy@chem.umass.edu. Phone: (413) 545-3486. Fax: (413) 545-4490.

ORCID

Jeanne A. Hardy: [0000-0002-3406-7997](https://orcid.org/0000-0002-3406-7997)

Funding

This work was supported by the National Institutes of Health (GM080532).

Notes

The authors declare no competing financial interest.

■ REFERENCES

- (1) Forbes, S. A., Bindal, N., Bamford, S., Cole, C., Kok, C. Y., Beare, D., Jia, M., Shepherd, R., Leung, K., Menzies, A., Teague, J. W., Campbell, P. J., Stratton, M. R., and Futreal, P. A. (2011) COSMIC: mining complete cancer genomes in the Catalogue of Somatic Mutations in Cancer. *Nucleic Acids Res.* 39, D945–950.
- (2) Lee, J. W., Kim, M. R., Soung, Y. H., Nam, S. W., Kim, S. H., Lee, J. Y., Yoo, N. J., and Lee, S. H. (2006) Mutational analysis of the CASP6 gene in colorectal and gastric carcinomas. *APMIS* 114, 646–650.
- (3) Pop, C., and Salvesen, G. S. (2009) Human caspases: activation, specificity, and regulation. *J. Biol. Chem.* 284, 21777–21781.
- (4) Yan, N., and Shi, Y. (2005) Mechanisms of apoptosis through structural biology. *Annu. Rev. Cell Dev. Biol.* 21, 35–56.
- (5) Fuentes-Prior, P., and Salvesen, G. S. (2004) The protein structures that shape caspase activity, specificity, activation and inhibition. *Biochem. J.* 384, 201–232.
- (6) Grutter, M. G. (2000) Caspases: key players in programmed cell death. *Curr. Opin. Struct. Biol.* 10, 649–655.
- (7) Inoue, S., Browne, G., Melino, G., and Cohen, G. M. (2009) Ordering of caspases in cells undergoing apoptosis by the intrinsic pathway. *Cell Death Differ.* 16, 1053–1061.
- (8) McIlwain, D. R., Berger, T., and Mak, T. W. (2013) Caspase functions in cell death and disease. *Cold Spring Harbor Perspect. Biol.* 5, a008656.
- (9) Earnshaw, W. C., Martins, L. M., and Kaufmann, S. H. (1999) Mammalian caspases: structure, activation, substrates, and functions during apoptosis. *Annu. Rev. Biochem.* 68, 383–424.
- (10) Srinivasula, S. M., Fernandes-Alnemri, T., Zangrilli, J., Robertson, N., Armstrong, R. C., Wang, L., Trapani, J. A., Tomaselli, K. J., Litwack, G., and Alnemri, E. S. (1996) The Ced-3:Interleukin 1b Converting Enzyme-like Homolog Mch6 and the Lamin-cleaving Enzyme Mch2a Are Substrates for the Apoptotic Mediator CPP32. *J. Biol. Chem.* 271, 27099–27106.
- (11) Slee, E. A., Harte, M. T., Kluck, R. M., Wolf, B. B., Casiano, C. A., Newmeyer, D. D., Wang, H. G., Reed, J. C., Nicholson, D. W., Alnemri, E. S., Green, D. R., and Martin, S. J. (1999) Ordering the cytochrome c-initiated caspase cascade: hierarchical activation of caspases-2, -3, -6, -7, -8, and -10 in a caspase-9-dependent manner. *J. Cell Biol.* 144, 281–292.
- (12) Klaiman, G., Champagne, N., and LeBlanc, A. C. (2009) Self-activation of Caspase-6 in vitro and in vivo: Caspase-6 activation does not induce cell death in HEK293T cells. *Biochim. Biophys. Acta, Mol. Cell Res.* 1793, 592–601.
- (13) Wang, X. J., Cao, Q., Liu, X., Wang, K. T., Mi, W., Zhang, Y., Li, L. F., LeBlanc, A. C., and Su, X. D. (2010) Crystal structures of human caspase 6 reveal a new mechanism for intramolecular cleavage self-activation. *EMBO Rep.* 11, 841–847.
- (14) Boatright, K. M., and Salvesen, G. S. (2003) Mechanisms of caspase activation. *Curr. Opin. Cell Biol.* 15, 725–731.
- (15) Suzuki, A., Kusakai, G., Kishimoto, A., Shimojo, Y., Miyamoto, S., Ogura, T., Ochiai, A., and Esumi, H. (2004) Regulation of caspase-6 and FLIP by the AMPK family member ARK5. *Oncogene* 23, 7067–7075.
- (16) Talanian, R. V., Quinlan, C., Trautz, S., Hackett, M. C., Mankovich, J. A., Banach, D., Ghayur, T., Brady, K. D., and Wong, W. W. (1997) Substrate specificities of caspase family proteases. *J. Biol. Chem.* 272, 9677–9682.
- (17) Ruchaud, S., Korfali, N., Villa, P., Kottke, T. J., Dingwall, C., Kaufmann, S. H., and Earnshaw, W. C. (2002) Caspase-6 gene disruption reveals a requirement for lamin A cleavage in apoptotic chromatin condensation. *EMBO J.* 21, 1967–1977.
- (18) Julien, O., Zhuang, M., Wiita, A. P., O'Donoghue, A. J., Knudsen, G. M., Craik, C. S., and Wells, J. A. (2016) Quantitative MS-based enzymology of caspases reveals distinct protein substrate specificities, hierarchies, and cellular roles. *Proc. Natl. Acad. Sci. U. S. A.* 113, E2001–2010.
- (19) Futreal, P. A., Coin, L., Marshall, M., Down, T., Hubbard, T., Wooster, R., Rahman, N., and Stratton, M. R. (2004) A census of human cancer genes. *Nat. Rev. Cancer* 4, 177–183.
- (20) Hanahan, D., and Weinberg, R. A. (2011) Hallmarks of cancer: the next generation. *Cell* 144, 646–674.
- (21) Frejlich, E., Rudno-Rudzinska, J., Janiszewski, K., Salomon, L., Kotulski, K., Pelzer, O., Grzebieniak, Z., Tarnawa, R., and Kielan, W. (2013) Caspases and their role in gastric cancer. *Advances in Clinical and Experimental Medicine: Official Organ Wroclaw Medical University* 22, 593–602.
- (22) Hosomi, Y., Gemma, A., Hosoya, Y., Nara, M., Okano, T., Takenaka, K., Yoshimura, A., Koizumi, K., Shimizu, K., and Kudoh, S. (2003) Somatic mutation of the Caspase-5 gene in human lung cancer. *Int. J. Mol. Med.* 12, 443–446.
- (23) Kim, Y. R., Kim, K. M., Yoo, N. J., and Lee, S. H. (2009) Mutational analysis of CASP1, 2, 3, 4, 5, 6, 7, 8, 9, 10, and 14 genes in gastrointestinal stromal tumors. *Hum. Pathol.* 40, 868–871.
- (24) Liu, B., Peng, D., Lu, Y., Jin, W., and Fan, Z. (2002) A novel single amino acid deletion caspase-8 mutant in cancer cells that lost proapoptotic activity. *J. Biol. Chem.* 277, 30159–30164.

- (25) Soung, Y. H., Jeong, E. G., Ahn, C. H., Kim, S. S., Song, S. Y., Yoo, N. J., and Lee, S. H. (2008) Mutational analysis of caspase 1, 4, and 5 genes in common human cancers. *Hum. Pathol.* 39, 895–900.
- (26) Soung, Y. H., Lee, J. W., Kim, H. S., Park, W. S., Kim, S. Y., Lee, J. H., Park, J. Y., Cho, Y. G., Kim, C. J., Park, Y. G., Nam, S. W., Jeong, S. W., Kim, S. H., Lee, J. Y., Yoo, N. J., and Lee, S. H. (2003) Inactivating mutations of CASPASE-7 gene in human cancers. *Oncogene* 22, 8048–8052.
- (27) Soung, Y. H., Lee, J. W., Kim, S. Y., Park, W. S., Nam, S. W., Lee, J. Y., Yoo, N. J., and Lee, S. H. (2004) Somatic mutations of CASP3 gene in human cancers. *Hum. Genet.* 115, 112–115.
- (28) Yoo, N. J., Lee, J. W., Kim, Y. J., Soung, Y. H., Kim, S. Y., Nam, S. W., Park, W. S., Lee, J. Y., and Lee, S. H. (2004) Loss of caspase-2, -6 and -7 expression in gastric cancers. *APMIS* 112, 330–335.
- (29) Soung, Y. H., Lee, J. W., Kim, S. Y., Jang, J., Park, Y. G., Park, W. S., Nam, S. W., Lee, J. Y., Yoo, N. J., and Lee, S. H. (2005) CASPASE-8 gene is inactivated by somatic mutations in gastric carcinomas. *Cancer Res.* 65, 815–821.
- (30) Devarajan, E., Sahin, A. A., Chen, J. S., Krishnamurthy, R. R., Aggarwal, N., Brun, A. M., Sapino, A., Zhang, F., Sharma, D., Yang, X. H., Tora, A. D., and Mehta, K. (2002) Down-regulation of caspase 3 in breast cancer: a possible mechanism for chemoresistance. *Oncogene* 21, 8843–8851.
- (31) Vaidya, S., Velazquez-Delgado, E. M., Abbruzzese, G., and Hardy, J. A. (2011) Substrate-induced conformational changes occur in all cleaved forms of caspase-6. *J. Mol. Biol.* 406, 75–91.
- (32) Pettersen, E. F., Goddard, T. D., Huang, C. C., Couch, G. S., Greenblatt, D. M., Meng, E. C., and Ferrin, T. E. (2004) UCSF Chimera—a visualization system for exploratory research and analysis. *J. Comput. Chem.* 25, 1605–1612.
- (33) Webb, B., and Sali, A. (2014) Protein structure modeling with MODELLER. *Methods Mol. Biol.* 1137, 1–15.
- (34) Velazquez-Delgado, E. M., and Hardy, J. A. (2012) Phosphorylation regulates assembly of the caspase-6 substrate-binding groove. *Structure* 20, 742–751.
- (35) Nandi, C. L., Singh, J., and Thornton, J. M. (1993) Atomic environments of arginine side chains in proteins. *Protein Eng., Des. Sel.* 6, 247–259.
- (36) Gallivan, J. P., and Dougherty, D. A. (1999) Cation- π interactions in structural biology. *Proc. Natl. Acad. Sci. U. S. A.* 96, 9459–9464.
- (37) Cowling, V., and Downward, J. (2002) Caspase-6 is the direct activator of caspase-8 in the cytochrome c-induced apoptosis pathway—absolute requirement for removal of caspase-6 prodomain. *Cell Death Differ.* 9, 1046–1056.
- (38) Ji, G. H., Li, M., Cui, Y., and Wang, J. F. (2014) The relationship of CASP 8 polymorphism and cancer susceptibility: a meta-analysis. *Cell. Mol. Biol. (Sarreguemines, Fr., Online)* 60, 20–28.
- (39) Soung, Y. H., Lee, J. W., Kim, S. Y., Jang, J., Park, Y. G., Park, W. S., Nam, S. W., Lee, J. Y., Yoo, N. J., and Lee, S. H. (2005) CASPASE-8 gene is inactivated by somatic mutations in gastric carcinomas. *Cancer Res.* 65, 815–821.
- (40) Mandruzzato, S., Brasseur, F., Andry, G., Boon, T., and van der Bruggen, P. (1997) A CASP-8 mutation recognized by cytolytic T lymphocytes on a human head and neck carcinoma. *J. Exp. Med.* 186, 785–793.
- (41) Park, H. L., Ziogas, A., Chang, J., Desai, B., Bessonova, L., Garner, C., Lee, E., Neuhausen, S. L., Wang, S. S., Ma, H., Clague, J., Reynolds, P., Lacey, J. V., Jr., Bernstein, L., and Anton-Culver, H. (2016) Novel polymorphisms in caspase-8 are associated with breast cancer risk in the California Teachers Study. *BMC Cancer* 16, 14.
- (42) Su, H., Bidere, N., Zheng, L., Cubre, A., Sakai, K., Dale, J., Salmena, L., Hakem, R., Straus, S., and Lenardo, M. (2005) Requirement for caspase-8 in NF- κ B activation by antigen receptor. *Science* 307, 1465–1468.
- (43) Bell, B. D., Leverrier, S., Weist, B. M., Newton, R. H., Arechiga, A. F., Luhrs, K. A., Morrisette, N. S., and Walsh, C. M. (2008) FADD and caspase-8 control the outcome of autophagic signaling in proliferating T cells. *Proc. Natl. Acad. Sci. U. S. A.* 105, 16677–16682.
- (44) Barbero, S., Mielgo, A., Torres, V., Teitz, T., Shields, D. J., Mikolon, D., Bogoyo, M., Barila, D., Lahti, J. M., Schlaepfer, D., and Stupack, D. G. (2009) Caspase-8 association with the focal adhesion complex promotes tumor cell migration and metastasis. *Cancer Res.* 69, 3755–3763.
- (45) Senft, J., Helfer, B., and Frisch, S. M. (2007) Caspase-8 interacts with the p85 subunit of phosphatidylinositol 3-kinase to regulate cell adhesion and motility. *Cancer Res.* 67, 11505–11509.
- (46) Lek, M., et al. (2016) Analysis of protein-coding genetic variation in 60,706 humans. *Nature* 536, 285–291.
- (47) Stupack, D. G. (2013) Caspase-8 as a Therapeutic Target in Cancer. *Cancer Lett.* 332, 133–140.
- (48) Ventura, J., Eron, S. J., Gonzalez-Toro, D. C., Raghupathi, K., Wang, F., Hardy, J. A., and Thayumanavan, S. (2015) Reactive Self-Assembly of Polymers and Proteins to Reversibly Silence a Killer Protein. *Biomacromolecules* 16, 3161–3171.
- (49) Robinson, D., et al. (2015) Integrative Clinical Genomics of Advanced Prostate Cancer. *Cell* 161, 1215–1228.
- (50) Pickering, C. R., et al. (2014) Mutational Landscape of Aggressive Cutaneous Squamous Cell Carcinoma. *Clin. Cancer Res.* 20, 6582–6592.
- (51) Bell, D., et al. (2011) Integrated genomic analyses of ovarian carcinoma. *Nature* 474, 609–615.
- (52) Crompton, B. D., et al. (2014) The Genomic Landscape of Pediatric Ewing Sarcoma. *Cancer Discovery* 4, 1326–1341.
- (53) Sharpe, H. J., et al. (2015) Genomic Analysis of Smoothed Inhibitor Resistance in Basal Cell Carcinoma. *Cancer Cell* 27, 327–341.
- (54) Durinck, S., et al. (2014) Spectrum of diverse genomic alterations define non-clear cell renal carcinoma subtypes. *Nat. Genet.* 47, 13–21.
- (55) Wang, K., et al. (2014) Whole-genome sequencing and comprehensive molecular profiling identify new driver mutations in gastric cancer. *Nat. Genet.* 46, 573–582.